

---

Archiv-Ex.:

FZR-131

April 1996

Preprint

*D. Henke, H. Tyrroff,  
H. Wirth and G. Zschornack*

**Output Maximization  
of a 7.25 GHz ECR Ion Source**

**Forschungszentrum Rossendorf e.V.**

Postfach 51 01 19 · D-01314 Dresden

Bundesrepublik Deutschland

Telefon (0351) 260 2987

Telefax (0351) 260 3285

E-Mail [tyrroff@fz-rossendorf.de](mailto:tyrroff@fz-rossendorf.de)

# Output Maximization of a 7.25 GHz ECR Ion Source

**D. Henke, H. Tyrroff**

FZ Rossendorf e. V., Institut für Ionenstrahlphysik und Materialforschung,  
POB 510119, D- 01314 Dresden, Germany

**H. Wirth, G. Zschornack**

Technische Universität Dresden, Institut für Kern- und Teilchenphysik,  
MommSENstr. 13, D-01062 Dresden, Germany

## 1. Introduction

The operating parameters of the Rossendorf 7.25 GHz ECR ion source [1,2] have been investigated in respect to maximize the current output for different ions, especially for the high charge states.

The main features of the ion source (s. fig.1) and the experimental setup are the following :

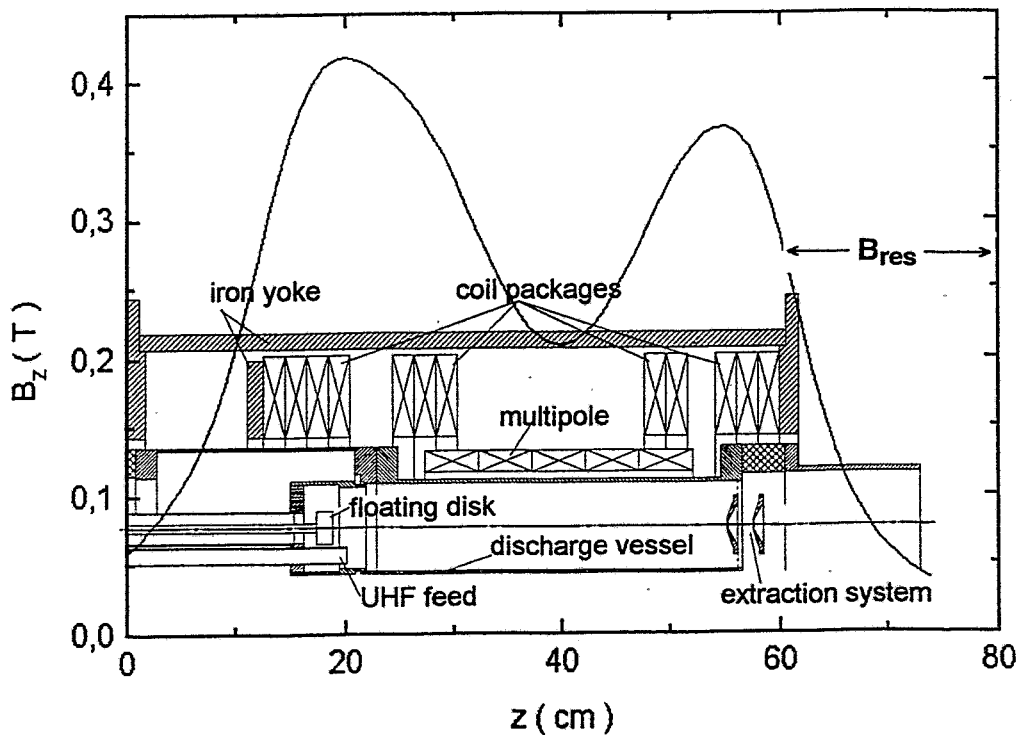


Figure 1: Scheme of the 7.25 GHz ECR ion source of the FZ Rossendorf

- single stage, floating disk supported discharge with UHF input power < 200 W ;
- air cooled plasma chamber of 83 mm diameter and 310 mm length;
- solenoid coil packages generating a mirror ratio of 2;
- Fe-Nd-B multipole (hexapole), creating the magnetic resonance flux density at a radius of about 35 mm;
- single gap ion acceleration;
- magnetic, double focusing q/A beam analyzer with an acceptance of about  $\pi \cdot 160$  mm mrad; beam probe and Faraday cup.

Gas pressure and gas composition, axial magnetic field and UHF power have been varied to maximize the ion output. In comparison to single stage devices with similar UHF frequency [3] the ion output of our machine is moderate and amounts to e.g.  $8 \mu\text{A}$  for  $\text{Ar}^{9+}$  or  $1.5 \mu\text{A}$  for  $\text{Xe}^{18+}$ . Basic parameters and limits of the source have been determined and the result of the optimization process is reproducible.

## 2. Influence of the gas pressure

The gas pressure has a strong influence on ionization and recombination [4]. The working gas is fed directly into the discharge vessel and the pressure is measured in the 4-way crosses positioned behind the ion source. Fig.2 illustrates the source behaviour for typical values of the magnetic mirror field excitation of 900 A and a UHF power of 75 W in the pressure region between  $0.5 \cdot 10^{-4}$  and  $2.5 \cdot 10^{-4}$  Pa.

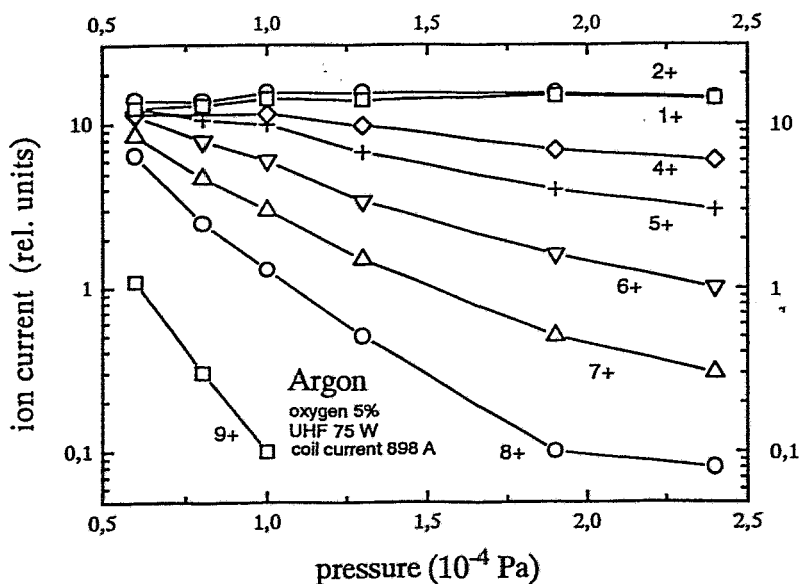


Figure 2: Pressure influence on the ion current for different charge states

Higher pressures of about  $2 \cdot 10^{-4}$  Pa were found to suppress the production of highly charged ions. Here the electron heating is inefficient because of the small free path length and dominating recombination processes. The output of highly charged ions increases down to pressure values below  $0.5 \cdot 10^{-4}$  Pa. In order to obtain maximum currents of highly charged ions additionally oxygen was mixed to argon and xenon, respectively up to pressures of approximately  $2 \cdot 10^{-4}$  Pa. At total pressures below  $5 \cdot 10^{-5}$  Pa the ion current is reduced because of particle lack. To minimize interference of isotopes with neighbouring  $q/A$ -ratios we used Ar, O and  $^{136}\text{Xe}$ .

### 3. Gas mixing

The physical effect of gas mixing has been discussed controversially since its discovery. A recently published model of ion confinement of magnetically trapped electrons in the electrostatic potential  $U_p$  predicts that the ion life time

$$\tau \propto \sqrt{A} \exp\left(\frac{qeU_p}{kT}\right)$$

depends on the mass  $A$ , the mean kinetic energy  $kT$  and the charge state  $q$  [5]. Assuming the ions are in thermodynamic equilibrium the confinement time of the added light gas (e.g. oxygen) is much shorter than that of the operating gas (e.g. argon). In this way this admixture carries away thermal energy and acts as coolant. It reduces the mean ion temperature and increases confinement time and charge state of the operating gas. In Tab.1 the effect of gas mixing is illustrated.

Table 1: Ion currents in  $\mu\text{A}$  extracted of Ar-O-plasmas with different argon content

| Ion species                         | 70 % Ar | 13 % Ar |
|-------------------------------------|---------|---------|
| Ar <sup>+</sup>                     | 15      | -       |
| Ar <sup>2+</sup>                    | 20      | -       |
| H <sub>2</sub> O <sup>+</sup>       | 1.2     | -       |
| OH <sup>+</sup>                     | 1.1     | -       |
| O <sup>+</sup>                      | 2.4     | 14      |
| N <sup>+</sup>                      | 1.1     | -       |
| Ar <sup>3+</sup>                    | 19      | 1       |
| C <sup>+</sup>                      | 1       | 1.8     |
| Ar <sup>4+</sup>                    | 15      | 1.8     |
| O <sup>2+</sup> & Ar <sup>5+</sup>  | 9.5     | 17      |
| Ar <sup>6+</sup>                    | 4.7     | 4.4     |
| Ar <sup>7+</sup>                    | 1.8     | 7       |
| O <sup>3+</sup>                     | -       | 13      |
| Ar <sup>8+</sup>                    | -       | 14      |
| Ar <sup>9+</sup>                    | -       | 8       |
| O <sup>4+</sup> & Ar <sup>10+</sup> | -       | 15      |
| Ar <sup>11+</sup>                   | -       | 1.0     |
| O <sup>5+</sup>                     | -       | 4.4     |

The change in the energy distribution of the high energetic part of the plasma electrons of the ECR discharge for different gas compositions was a key to understand the gas mixing effect. The experimental method to determine the electron energy distribution using the bremsstrahlung emitted by the plasma is described in [6]. Addition of oxygen to an argon discharge decreases the density of the total bremsstrahlung emission to about 40 % but increases the density of electrons with energies higher than 1 keV by the factor of two. Further, the energy loss per electron and time is reduced to 20 % compared to the pure argon regime if magnetic field, microwave power and gas pressure are not changed. In this way, the increased number of energetic electrons enhances the formation of higher ion charge states.

#### 4. Influence of the axial magnetic field

A typical axial magnetic flux density distribution of the given source for an excitation current of 820 A is demonstrated in fig. 1.

The magnetic flux density for electron resonance is indicated in fig. 1. In the case of increasing the flux density lower magnetic field gradient regions move to the resonance region and the coupling of electromagnetic energy to the plasma electrons is improved. This explains the results demonstrated in fig. 3: the output of highly charged ions generally increases with increasing magnetic field strength.

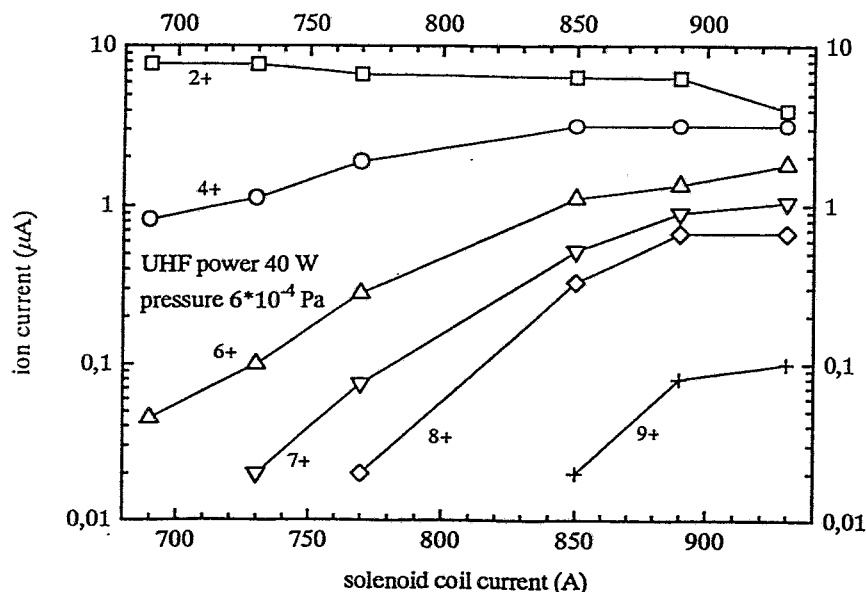


Figure 3: Argon ion currents of different charge states vs. solenoid coil current

A further increase of the highly charged ion output is expected for still higher magnetic flux densities. The electrical and thermal limits of the power supply are reached for solenoid currents of about 950 A. However, we have the possibility to redesign the magnetic circuit of the ion source. In this way maximal flux density and mirror ratio can be increased.

At reduced pressure favourable for creating high charge states, the mentioned general behaviour is often disturbed at the maximum of the achievable currents. Here instabilities occur. These instabilities have been observed using a beam probe and following the beam hash on the oscilloscope. Fig. 4 illustrates the ion current output in flux density regions creating beam hash.

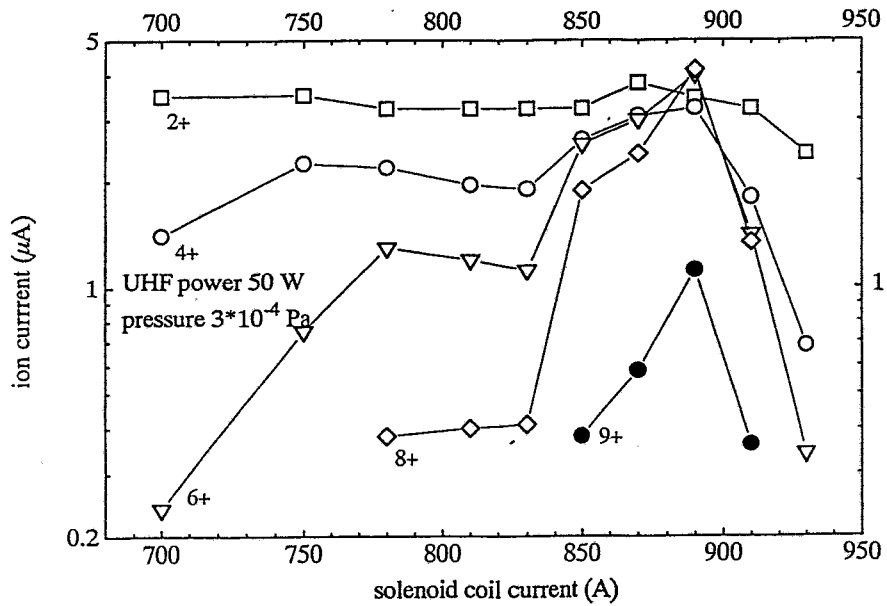


Figure 4: Ion current fluctuations and critical solenoid coil currents

## 5. UHF power

The output of  $\text{Ar}^{9+}$  as a function of the UHF power for an Ar discharge well suited for the creation of high charge states is demonstrated in fig. 5.

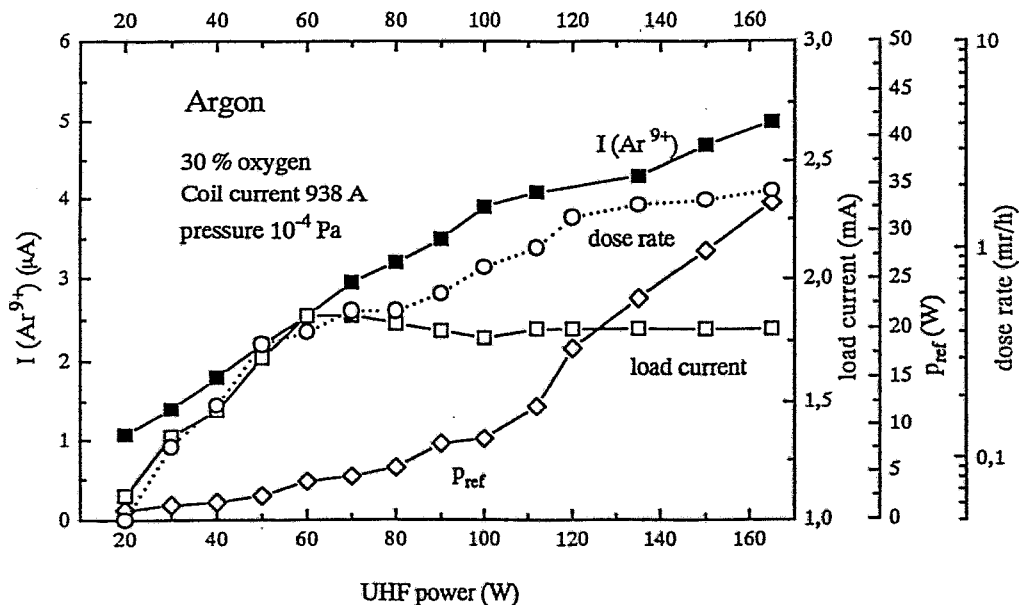


Figure 5:  $\text{Ar}^{9+}$  output, load current, reflected UHF power and Bremsstrahlung dose rate several meters away from the source versus UHF power

The figure shows that for a power > 80 W the load current of the extraction voltage does not increase furthermore and the reflected power starts raising much stronger. We estimated the total ion current emitted from the source to be one half of the load current. From fig. 5 we conclude that the total ion current emitted by the plasma approaches saturation at P<sub>UHF</sub> about 80 W at the given pressure and flux density. However, the output of a rather highly charged beam component as Ar<sup>9+</sup> and the emitted Bremsstrahlung still continue growing beyond P<sub>UHF</sub> = 80 W. The UHF power is now distributed to the more energetic electrons what enhances higher charge states and intensity of Bremsstrahlung. The total ion current density of our source amounts to  $j^+ = 1...2 \text{ mA/cm}^2$ . With an ion density  $n^+$  of the order of  $10^9$  per  $\text{cm}^3$  obtained from characteristic X-ray spectra of a xenon plasma [7] we estimate a mean electron temperature  $T_e$  of all electrons, contributing to the ion current, using

$$j^+ = 0.4en^+ \sqrt{\frac{kT_e}{m^+}}$$

in the order of 1 keV ( $m^+$ : atomic weight of the ions being emitted). From measurements of Bremsstrahlung emitted by our source we know [6] that the high energetic part of the energy distribution function of the plasma electrons consists of a warm and a hot component with maximal energies of 3 and 25 keV, respectively. The above estimated value of 1 keV represents a mean figure enclosing all electrons being involved in the ECR discharge.

In comparison to 14.5 GHz ECR ion sources (s.e.g. [8]) gas pressure and ion density of our source are rather low. This explains the moderate ion output.

Looking at fig. 5 one expects that the highly charged output should increase if still more power is fed to the source. Unfortunately, the insufficient air cooling of the our discharge vessel limits the UHF power level to values below 300 W.

## 6. Optimization results

To maximize the output of different charge states it is not sufficient to follow only one of the given relationships in figs. 2, 3, 4, 5. instead, it is necessary to change the whole operation group of parameters repeatedly. In order to obtain the maximum current of a certain charge state, this procedure was simplified by fixing different pressure values of the working gas and varying the gas pressure of the cooling gas only. For this sets of gas pressures the optimal values of axial magnetic field and microwave power have to be found.

Figures 6 and 7 show the result of the Ar and the <sup>136</sup>Xe optimization for charge states between 1 and 20. The operating parameters belonging to several maximized charge states of Ar and Xe are indicated too. Obviously, to shift the maximum output to higher charge states UHF power and mirror field have to be increased at reduced working gas pressure. Exclusions from this rule are due to the attempt to avoid beam hash.

Quantitatively we established, that for Ar and Xe the admixture of oxygen as coolant is advantageous for charge states >6. Especially for argon the optimum gas pressure has to be reduced to about 1/10 if one changes from single charged ions to  $q=11$ . The optimum UHF power increases from several Watts for the lowest charge states to  $P > 100$  W for the highest ones. For the highest charge states the total ion



beam contains only several percent of the working gas, about 50 % of the coolant oxygen and a significant part of hydrogen which may act as coolant for oxygen.

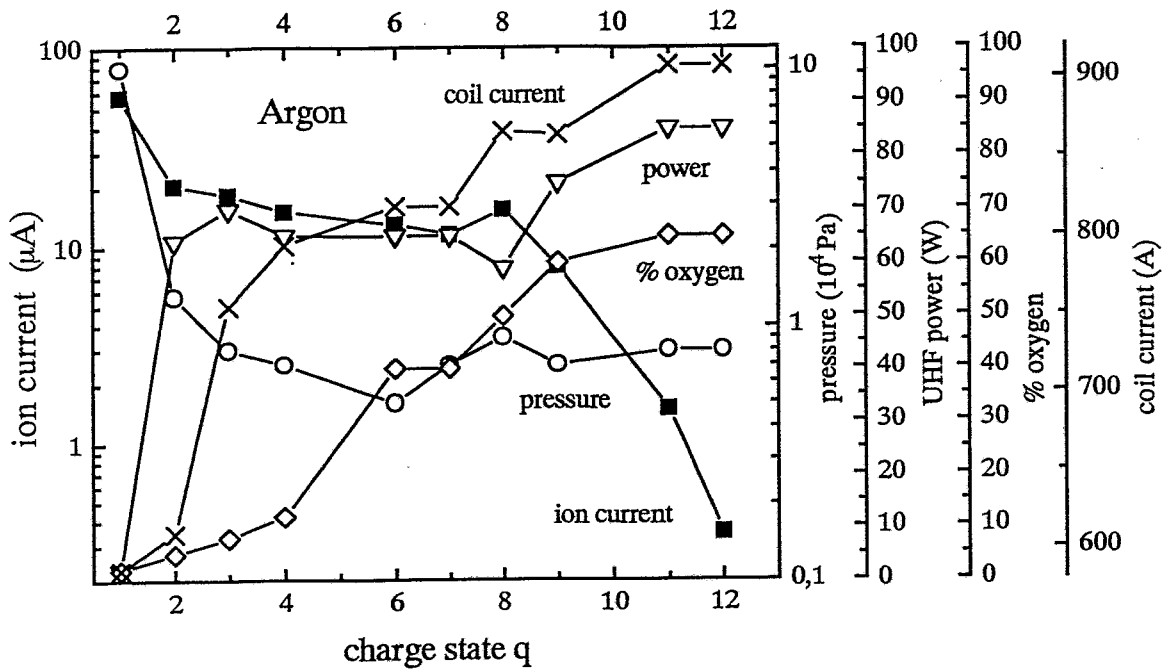


Figure 6: Maximized current output of argon ions and corresponding operating parameters for different charge states

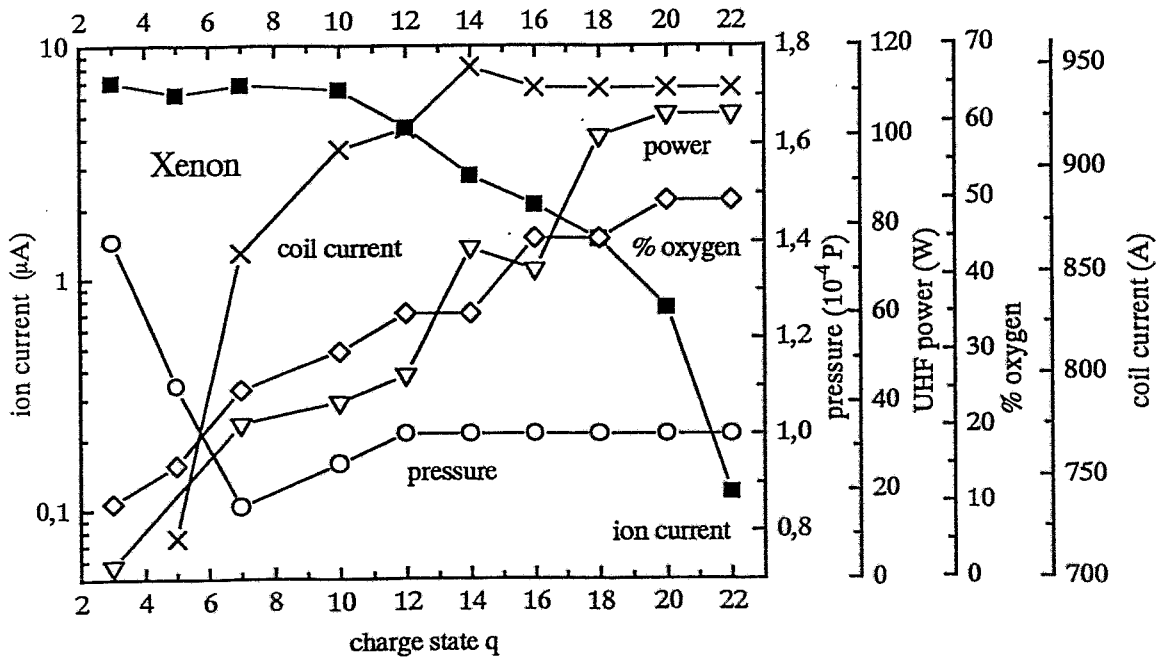


Figure 7: Maximized current output of xenon ions and corresponding operating parameters for different charge states

To obtain reproducible optimization results it is important to degas the source by the maximum UHF power in advance.

The broad range of charge states in the xenon ion spectrum gives ideal prerequisites for investigations of the charge state distribution depending on special source operation parameters. This is demonstrated in Fig.8. It contains the ion current spectra for maximum ion currents of a certain charge state. One recognizes that the capability of the source is reached when a shift of the charge state distribution to higher charge states is no more connected with an increase of ion currents. In Fig. 8 this is the case for  $q=18$ .

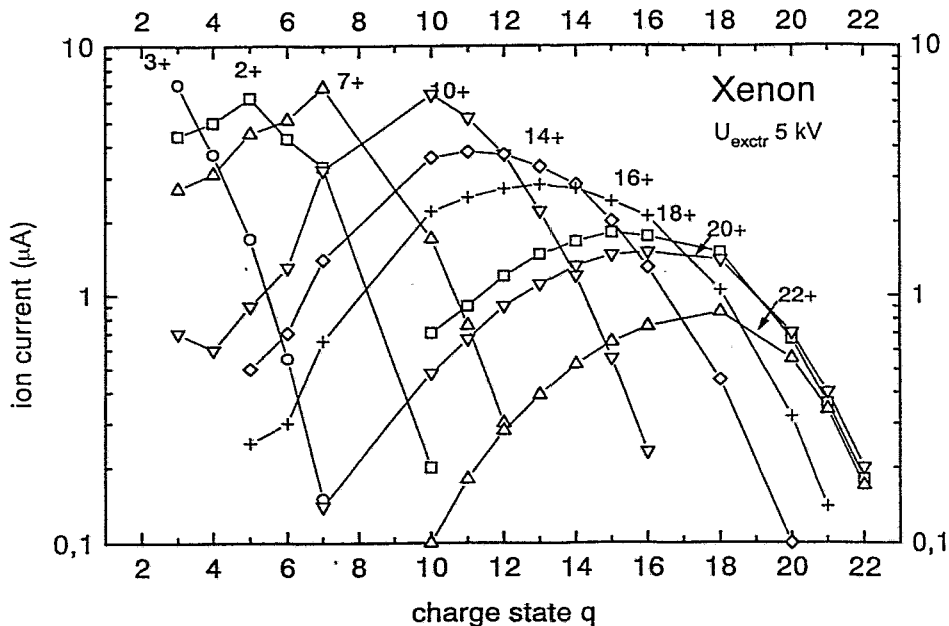


Figure 8: Experimental results of xenon ion current optimization. The indicated charge states were tried to maximize

## 7. Conclusion

The ion output of our single stage, low plasma density ECR ion source can be maximized for a wide range of charge states by optimizing the operation parameters of the source. Especially for gaseous feed materials gas mixing is effective to create highly charged ions. The output of our source is limited by discharge instabilities arising at low pressure - strong magnetic longitudinal field regimes. An enhancement of the UHF power of about 200 W is expected to increase the highly charged output. This needs to replace the non sufficient air cooling of the source. A redesign of the magnetic circuit of the mirror field can improve the effectivity of the mirror field and a stronger multipole will move the resonance zone closer to the magnetic axis of the discharge vessel. Both measures will improve the higher charge state output.

We thank G. Franz, P. Hartmann and F. Nötzold for technical assistance and R. Hentschel who participated in an early stage of the work. The stimulating interest of Prof. E. Wieser and Prof. E. Salzborn is deeply acknowledged. Support by Bundesminister für Forschung und Technologie (Contract No.06 DD11), Sächsisches Staatsministerium für Wissenschaft und Kunst (contract No. 7541.83-FZR/320) and Volkswagen Stiftung (contracts No. I/66139 and I/65890) is greatly appreciated.

## References

- [1] L. Friedrich, E. Huttel, R. Hentschel and H. Tyrroff,  
Proc. of the 11th Intern. Workshop on ECR Ion Sources, May 1993,  
Groningen, (1993) 19.
- [2] D. Henke, H. Tyrroff, R. Grötzschel, H. Wirth,  
Slow, highly charged ions from a 7.25 GHz ECR ion source  
Nuclear Instruments & Methods B98, (1995) 528.
- [3] D. K. Bose and T. A. Antaya,  
Proc. of the Intern. Conf. ECR Ion Sources, Dec. 1987, East Lansing, (1987)  
371.
- [4] I. Steinert, G.D. Shirkov and G. Zschornack,  
NIM A314, (1992) 602.
- [5] G.D. Shirkov and G. Zschornack,  
Nuclear Instruments & Methods B95, (1995) 527.
- [6] R. Friedlein, S. Herpich, H. Hiller, H. Wirth, G. Zschornack, H. Tyrroff,  
Physics of Plasmas, 2 (1995) 1.
- [7] R. Friedlein, S. Herpich, U. Lehnert, H. Tyrroff, C. Zippe, G. Zschornack,  
Nuclear Instruments & Methods B98, (1995) 585.
- [8] M. Schlapp, R. Trassl, A. Heyer and E. Salzborn,  
Nuclear Instruments & Methods B98, (1995) 521.